Two different features of discharge of equatorial upper ocean heat content related to El Nino events

doi: 10.1029/2005GL024832

Two different features of discharge of equatorial upper ocean heat content related to El Niño events

Takuya Hasegawa,[1] Takanori Horii,[2] and Kimio Hanawa[2]

Received 3 October 2005; revised 6 December 2005; accepted 9 December 2005; published 24 January 2006.

[1] Oceanic and atmospheric anomaly fields in the tropical Pacific are investigated to extract some characteristics from twelve El Niño events in the past 49 years. The results show that entire equatorial upper ocean heat content (*Teq*) is discharged after the mature phase of seven El Niño events (*A-type* events), while *Teq* is not well discharged in other five events (*B-type* events). Furthermore, *A-type* events generally have larger amplitudes of tropical oceanic and atmospheric anomalies than *B-type* events. In addition, the durations of *A-type* events are longer than those of *B-type* events. It is also found that *A-type* events accompany large positive wind stress curl anomaly and resultant poleward Sverdrup transport in the tropical South Pacific after the mature phase of El Niño events, while *B-type* events do not. This appearance of large positive wind stress anomaly should be one of the reasons why *Teq* is well discharged in *A-type* events. **Citation:** Hasegawa, T., T. Horii, and K. Hanawa (2006), Two different features of discharge of equatorial upper ocean heat content related to El Niño events, *Geophys. Res. Lett.*, *33*, L02609, doi:10.1029/2005GL024832.

1. Introduction

[2] Sea surface temperature (SST) and atmospheric anomaly fields related to El Niño/Southern Oscillation (ENSO) events have been well documented (e.g., *Bjerknes* [1966], among others). After the 1990s, observed subsurface temperature data sets have been available, and several authors have analyzed upper ocean heat content (OHC) or isothermal depth anomalies. The previous studies [e.g., *Kessler*, 1990] have been pointed out propagating OHC anomalies in the tropical North Pacific, which supports the idea of a delayed action oscillator model [*Suarez and Schopf*, 1988], western Pacific oscillator model [*Weisberg and Wang*, 1997] and air-sea coupled eastward propagations so-called ''slow mode'' [e.g., *Hirst*, 1988]. It has been also pointed out that, in general, OHC anomaly spatially averaged in the entire equatorial Pacific, *Teq*, leads to SST anomaly in the central and eastern equatorial Pacific by about one fourth of the ENSO period. That is, *Teq* is discharged during the El Niño events [*Meinen and McPhaden*, 2000; *Kessler*, 2002; *Hasegawa and Hanawa*, 2003a]. This phase relationship is in line with that expected by a recharge-discharge oscillator model [*Jin*, 1996, 1997a, 1997b].

[3] However, it is not fully understood whether or not *Teq* is adequately discharged in all El Niño events, and how a behavior of *Teq* relates with characteristics of El Niño events. The purpose of the present study is to investigate a behavior of *Teq* and its relationship to characteristics associated with El Niño events, such as magnitude, duration, spatial distribution patterns of oceanic and atmospheric anomaly fields.

2. Data Used and Definition of El Niño Event

[4] In the present study, the quasi-global subsurface ocean temperature data set prepared by Scripps Institution of Oceanography [*White*, 1995] is used to calculate OHC. In this study, vertically averaged temperature from the sea surface to the depth of 300 m is used as a proxy for OHC. The analysis region is the Pacific Ocean (30°S–60°N) with a 2° × 5° grid point, and the analysis period is 49 years from January 1955 to December 2003.

[5] We also use the SST data set of *Smith and Reynolds* [2003]. In addition, wind stress data set from the National Centers for Environmental Prediction/National Center for Atmospheric Research (NCEP/NCAR) is used [*Kalnay et al.*, 1996]. For all variables, monthly anomalies are calculated by subtracting monthly climatologies from 1961 to 1990. Finally, a 5-month running mean filter is adopted for all variables in order to remove an intraseasonal variation such as Madden-Julian Oscillation [e.g., *Madden and Julian*, 1971].

[6] In this study, we define an El Niño event by using a 5-month running mean Niño-3 index (SST anomaly averaged over the region of [5°S–5°N, 150°W–90°W]). If monthly averaged Niño-3 index exceeds 0.5°C for longer than five months, the event is defined as an El Niño event. Such a definition for El Niño events is in line with that of JMA (Japan Meteorological Agency). The month when the Niño-3 index initially exceeds (falls) 0.5°C is regarded as the onset (termination) month, and the duration of the El Niño event is defined as the time length from the onset to the termination.

3. Results

[7] Figures 1a and 1b show trajectory plots of the OHC anomaly averaged over the entire equatorial Pacific (5°S–5°N, 130°E–90°W; *Teq*) and Niño-3 index for the 49-year period. It is ascertained that even if the latitudes of the above definition for *Teq* are changed from 3°S–3°N to 7°S–7°N, the main results are not changed. Based on the behavior of the trajectories, we classify the El Niño events into two types. That is, one type is an El Niño event whose trajectory at the termination is in the second quadrant of the diagram. This is the case that *Teq* is sufficiently

[1]Meteorological Research Institute, Japan Meteorological Agency, Tsukuba, Japan.
[2]Department of Geophysics, Tohoku University, Sendai, Japan.

0094-8276/06/2005GL024832$05.00

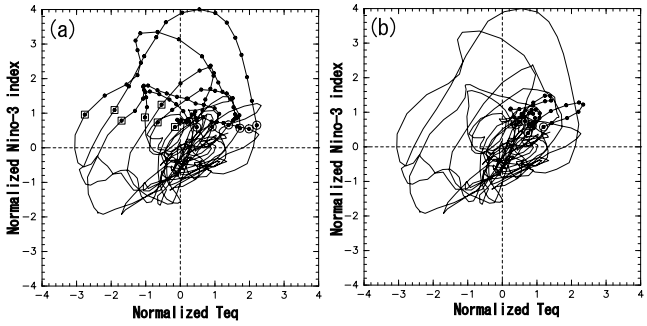

Figure 1. (a) Trajectory plots between *Teq* and Niño-3 index. Variables are normalized by the standard deviations. Closed circles indicate trajectories for El Niño events belonging to *A-type* events (see text), and open circles (squares) show onsets (terminations) of El Niño events. (b) Same as (a) but for *B-type* events.

discharged to become negative anomaly after the mature phase of El Niño (Figure 1a). The other is an El Niño event whose trajectory is not in the second quadrant: *Teq* is not discharged sufficiently and remains positive anomaly (Figure 1b). Hereafter, we call the El Niño events shown in Figure 1a '*A-type*' events, and those in Figure 1b '*B-type*' events. During the analysis period from 1955 to 2003, twelve El Niño events are defined, and seven El Niño events occurring in 1965/66, 1968/69, 1972/73, 1982/83, 1986/87, 1991/92 and 1997/98 are classified into *A-type* events, while the other five El Niño events occurring in 1957/58, 1963/64, 1976/77, 1994/95 and 2002/03 are classified into *B-type* events. Figure 1 also tells us that the *A-type* events have larger amplitudes of both Niño-3 index and *Teq* than those of the *B-type* events.

[8] Figure 2a shows scatter plots between *Teq* at the termination and the maximum value of the Niño-3 index in individual El Niño events. We can see that the six of the seven *A-type* events except for 1968/1969 event take the maximum values of the Niño-3 index from about 1.5°C to 3.0°C, while those of *B-type* events do around 1.0°C. Figure 2b is same as Figure 2a but the duration of an El Niño event. We can see that the durations of *A-type* events are from 10 to 18 months, while those of *B-type* events are

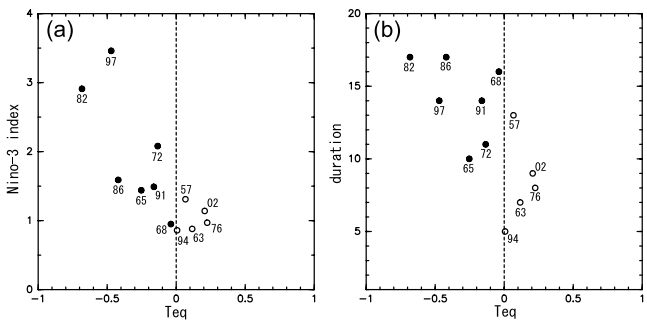

Figure 2. (a) Scatter plots between *Teq* at the termination and maximum value of Niño-3 index (°C). The attached numeral such as '97' means the El Niño event starting in 1997, and so on. Closed (open) circles denote the *A (B)-type* events. (b) Same as (a) but duration of El Niño events (month).

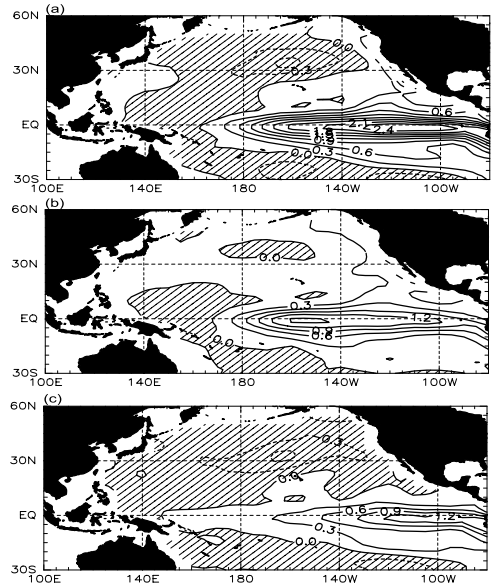

Figure 3. (a) A composite map of SST anomaly (°C) during *A-type* events. (b) Same as (a) but for *B-type* events. (c) Difference between (a) and (b).

from five to nine months except for the 1957/58 event. Therefore, it can be said that magnitudes of oceanic thermal anomalies of *A-type* events are larger than those of *B-type* events, and durations of *A-type* events are longer than those of *B-type* events, in general.

[9] Next, we show SST anomalies in the Pacific basin averaged during *A-type* events, *B-type* events and a difference between the two in Figures 3a, 3b, and 3c, respectively. It is clear that amplitudes of SST anomalies of *A-type* events are larger than those of *B-type* events in the equatorial Pacific, especially in the eastern equatorial Pacific as expected from Figures 1 and 2. *A-type* events reveal a well-known SST anomaly pattern of El Niño events, magnitudes of which are much stronger than *B-type* events. Figure 4 is same as Figure 3 but OHC anomalies instead of

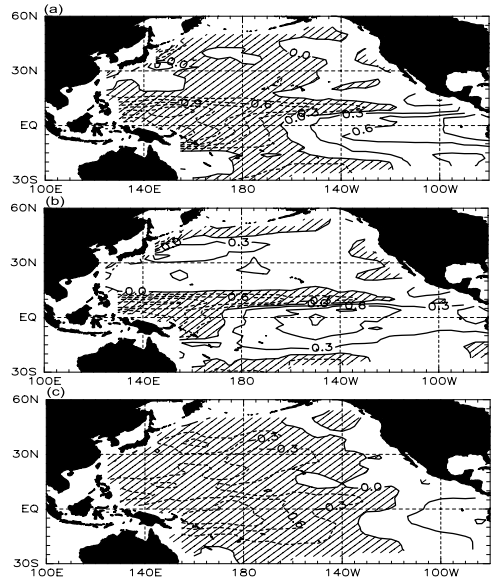

Figure 4. Same as Figure 3 but OHC anomaly (°C).

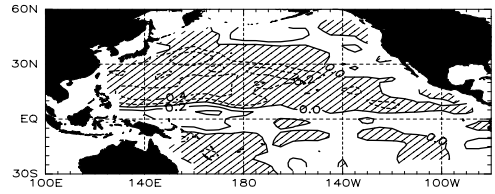

Figure 5. Same as Figure 4c but at the onset month.

SST anomalies. Figure 4 shows that *A-type* events have large magnitudes of positive and negative OHC anomalies in the eastern equatorial Pacific and in the western equatorial Pacific, respectively. This is clear evidence that the zonal sea-saw pattern of equatorial OHC anomalies related to the El Niño events [e.g., *Meinen and McPhaden*, 2000; *Hasegawa and Hanawa*, 2003a] are more dominant in the *A-type* events than in the *B-type* events.

[10] Figure 4 also shows that *Teq* in *A-type* events are colder than those of *B-type* events. At the onset month, however, equatorial OHC are not so different between *A-type* and *B-type* events as shown in Figure 5. However, negative OHC anomalies are situated in the off-equatorial tropical North Pacific (10°N–20°N, 130°E–180°) at the onset month in both *A-type* and *B-type* events (not shown here), and the negative OHC anomalies are larger in *A-type* events than *B-type* events (Figure 5). As pointed out in the previous studies [e.g., *Kessler*, 1990; *Hasegawa and Hanawa*, 2003a; *Weisberg and Wang*, 1997], the negative OHC anomalies in the off-equatorial North Pacific at onset can lead a reduction of equatorial OHC anomalies by their propagation toward the western equatorial Pacific and/or by changing atmospheric conditions which cause cold Kelvin waves in the western equatorial Pacific. That may be one of the reasons why *Teq* of *A-type* events become less than that of *B-type* events.

[11] In addition to the oceanic anomalies, atmospheric anomaly fields are also investigated to reveal the difference between *A-type* and *B-type* events. Wind stress anomalies of

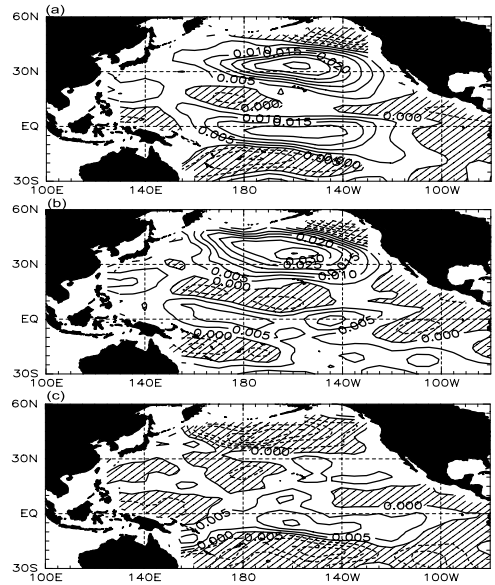

Figure 6. Same as Figure 3 but zonal wind stress anomaly (Nm^{-2}).

A-type events show larger positive zonal wind stress anomalies along the equator and larger negative anomalies in the off-equatorial tropical South Pacific centered in 15°S than *B-type* events (Figure 6). The tropical North Pacific does not show such a large difference of wind stress between *A-type* and *B-type* events. The larger meridional shear of the zonal wind stress anomaly in the tropical South Pacific during *A-type* events suggests that, after the mature phase of an El Niño event, *A-type* events accompany larger cyclonic wind stress curl anomalies in the tropical South Pacific than *B-type* events. Indeed, amplitudes of wind stress curl anomalies averaged over the tropical South Pacific after the mature phase of El Niño events are generally larger during *A-type* events than *B-type* events (Figure 7a).

[12] These cyclonic wind stress curl fields in the tropical Pacific may induce different Sverdrup transports between *A-type* and *B-type* events in the tropical South Pacific. In fact, Figure 7b shows that after mature phase of El Niño events, five of seven *A-type* events show large poleward Sverdrup transports (from −25 to −5 Sv) in the off-equatorial tropical South Pacific. On the other hand, *B-type* events show smaller transport (from −5 to +10 Sv) and in some cases, direction of Sverdrup transports is equatorward. According to the recharge-discharge oscillator model (hereafter '*RO model*'), positive wind stress curl anomalies in the off-equatorial tropical Pacific occur during an El Niño event, and they cause poleward Sverdrup transports, so that the *Teq* tends to discharge and then the on-going El Niño event moves to its termination. Therefore, it can be said that since the *A-type* events are accompanied by larger cyclonic wind stress curl anomalies and poleward Sverdrup transports in the tropical South Pacific after the mature phase, *Teq* is more discharged in *A-type* events rather than *B-type* events.

4. Summary and Discussion

[13] In the present study, we have shown the existence of two types of El Niño events, based on the trajectory analysis of *Teq* and Niño-3 index. *A-type* events show that *Teq* is sufficiently discharged to display negative anomaly at the termination of El Niño event, as opposed to *B-type* events.

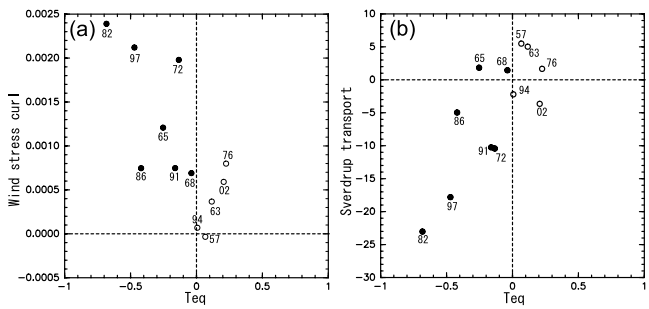

Figure 7. (a) Same as Figure 2a but wind stress curl anomaly ($Nm^{-3}s$) averaged over the tropical South Pacific (10°S–5°S, 140E°–90°W) in three months after the mature phase of El Niño event. (b) Same as (a) but Sverdrup transport (Sv) at [10°S, 160°E] three months after the mature phase of El Niño event. Positive (negative) values mean an equatorward (poleward) transport.

The present results also show that magnitudes (durations) of *A-type* events are larger (longer) than those of *B-type* events. In addition, large signals of wind stress curl anomaly and Sverdrup transport appear in the off-equatorial tropical South Pacific, during *A-type* events. That can lead to the discharge of equatorial OHC during El Niño events via poleward Sverdrup transport, and it is well consistent with the idea of the *RO model*. On the other hand, *B-type* events do not show such large wind stress curl anomaly and Sverdrup transport in the tropical South Pacific. In contrast to the tropical South Pacific, the tropical North Pacific does not show a large difference of wind stress anomalies between *A-type* and *B-type* events. So, it can be said that the tropical South Pacific is one of the key regions that is responsible for modulating *Teq* discharge.

[14] Furthermore, it is suggested that negative OHC anomalies in the off-equatorial western North Pacific of *A-type* events found at onset might contribute to the termination of El Niño events than *B-type* events. The off-equatorial OHC anomalies may be due to a local Ekman pumping as suggested by *Kessler* [1990], and might be also related to the western Pacific oscillator theory that emphasizes a role of off-equatorial western Pacific. Therefore, the present results also suggest that a unified oscillator model [*Wang*, 2001], which includes various ENSO mechanisms such as the *RO model*, western Pacific oscillator model and others, might be related to the modulation of *Teq* and ENSO characteristics.

[15] Finally, we wish to discuss the difference of El Niño to La Niña cycles in the two types. It is found that six of seven *A-type* events can go to La Niña events, and three of five *B-type* events can. It implies that the *A-type* events in which poleward Sverdrup transports discharge *Teq* well, can be followed by La Niña events in general, and some of *B-type* events can also be followed by them without such meridional Sverdrup transports. One possible reason is an anomalous zonal advection of mean SST which may serve as a phase transition mechanism as expected from a modified *RO model* [*Jin and An*, 1999]. Therefore, it can be concluded that the *RO model* is not complete to explain all of the El Niño to La Niña cycles. The *RO model* can only explain the strong and slow cycles of *A-type* events, and a different mechanism other than the *RO model*, the modified *RO model*, or effect of local wind variation in the equatorial Pacific [e.g., *Tziperman et al.*, 1997; *Harrison and Vecchi*, 1999; *McPhaden*, 2004] might explain the weak and fast cycles of *B-type* events. To explore mechanisms associated with the *B-type* events is the next target. Roles of seasonal phase locking of ENSO [e.g., *Xie*, 1995; *Tziperman et al.*, 1997; *Horii and Hanawa*, 2004], the regime shift [e.g., *Nitta and Yamada*, 1989; *Trenberth*, 1990; *Yasunaka and Hanawa*, 2005], and ENSO-like quasi-decadal variation of OHC anomalies [e.g., *Luo and Yamagata*, 2001; *Hasegawa and Hanawa*, 2003b; *White et al.*, 2003] in affecting *Teq* will be also explored in future works.

[16] **Acknowledgments.** The authors wish to express their sincere thanks to members of the Oceanographic Research Department at Japan Meteorological Agency/Meteorological Research Institute and Physical Oceanography Group at Tohoku University for their useful discussions. The authors also wish to deeply thank F.-F. Jin for his comments and suggestions that helped to improve our original manuscript. The manuscript was also improved through the help of the anonymous reviewer. The first author (Takuya Hasegawa) is financially supported by Research Fellowships of the Japan Society for the Promotion of Science for Young Scientists. The second author (Takanori Horii) is financially supported by the Earth Science 21st Century Center-Of-Excellence (COE) program at Tohoku University.

References

Bjerknes, J. (1966), A possible response of the atmospheric Hadley circulation to equatorial anomalies of ocean temperature, *Tellus*, *18*, 820–829.
Harrison, D. E., and G. A. Vecchi (1999), On the termination of El Niño, *Geophys. Res. Lett.*, *26*, 1593–1596.
Hasegawa, T., and K. Hanawa (2003a), Heat content variability related to ENSO events in the Pacific, *J. Phys. Oceanogr.*, *33*, 407–421.
Hasegawa, T., and K. Hanawa (2003b), Decadal-scale variability of upper ocean heat content in the tropical Pacific, *Geophys. Res. Lett.*, *30*(6), 1272, doi:10.1029/2002GL016843.
Hirst, C. H. (1988), Slow instabilities in tropical ocean basin-global atmosphere models, *J. Atmos. Sci.*, *45*, 830–852.
Horii, T., and K. Hanawa (2004), A relationship between timing of El Niño onset and subsequent evolution, *Geophys. Res. Lett.*, *31*, L06304, doi:10.1029/2003GL019239.
Jin, F.-F. (1996), Tropical ocean-atmosphere interaction, the Pacific cold tongue, and the El Niño-Southern Oscillation, *Science*, *274*, 76–78.
Jin, F.-F. (1997a), An equatorial ocean recharge paradigm for ENSO. part I: Conceptual model, *J. Atmos. Sci.*, *54*, 811–829.
Jin, F.-F. (1997b), An equatorial ocean recharge paradigm for ENSO. part II: A stripped-down coupled model, *J. Atmos. Sci.*, *54*, 830–847.
Jin, F.-F., and S.-I. An (1999), Thermocline and zonal advective feedbacks within the equatorial ocean recharge oscillator model for ENSO, *Geophys. Res. Lett.*, *26*, 2989–2992.
Kalnay, E., et al. (1996), The NCEP/NCAR 40-year reanalysis project, *Bull. Am. Meteorol. Soc.*, *77*, 437–471.
Kessler, W. S. (1990), Observations of long Rossby waves in the northern tropical Pacific, *J. Geophys. Res.*, *95*, 5183–5217.
Kessler, W. S. (2002), Is ENSO a cycle or a series of events?, *Geophys. Res. Lett.*, *29*(23), 2125, doi:10.1029/2002GL015924.
Luo, J., and T. Yamagata (2001), Long-term El Niño-Southern Oscillation (ENSO)-like variation with special emphasis on the South Pacific, *J. Geophys. Res.*, *106*, 22,211–22,227.
Madden, R. A., and P. R. Julian (1971), Detection of a 40–50 day oscillation in the zonal wind in the tropical Pacific, *J. Atmos. Sci.*, *28*, 702–708.
McPhaden, M. J. (2004), Evolution of the 2002/2003 El Niño, *Bull. Am. Meteorol. Soc.*, *85*, 677–695.
Meinen, C. S., and M. J. McPhaden (2000), Observations of warm water volume changes in the equatorial Pacific and their relationship to El Niño and La Niña, *J. Clim.*, *13*, 3551–3559.
Nitta, T., and S. Yamada (1989), Recent warming of tropical sea surface temperature and its relationship to the Northern Hemisphere circulation, *J. Meteorol. Soc. Jpn.*, *67*, 375–383.
Smith, T. M., and R. W. Reynolds (2003), Extended reconstruction of global sea surface temperatures based on COADS data (1854–1997), *J. Clim.*, *16*, 1495–1510.
Suarez, M. J., and P. S. Schopf (1988), A delayed action oscillator for ENSO, *J. Atmos. Sci.*, *45*, 3283–3287.
Trenberth, K. E. (1990), Recent observed interdecadal climate changes in the Northern Hemisphere, *Bull. Am. Meteorol. Soc.*, *71*, 933–988.
Tziperman, E., S. E. Zebiak, and M. A. Cane (1997), Mechanisms of seasonal-ENSO interaction, *J. Atmos. Sci.*, *54*, 61–71.
Wang, C. (2001), A unified oscillator model for the El Niño-Southern Oscillation, *J. Clim.*, *14*, 98–115.
Weisberg, R. H., and C. Wang (1997), A western Pacific oscillator paradigm for the El Niño-Southern Oscillation, *Geophys. Res. Lett.*, *24*, 779–782.
White, W. B. (1995), Design of a global observing system for gyre-scale upper ocean temperature variability, *Prog. Oceanogr.*, *36*, 169–217.
White, W. B., Y. M. Tourre, M. Barlow, and M. Dettinger (2003), A delayed action oscillator shared by biennial, interannual, and decadal signals in the Pacific Basin, *J. Geophys. Res.*, *108*(C3), 3070, doi:10.1029/2002JC001490.
Xie, S.-P. (1995), Interaction between the annual and interannual variations in the equatorial Pacific, *J. Phys. Oceanogr.*, *25*, 1930–1941.
Yasunaka, S., and K. Hanawa (2005), Regime shift in the global sea-surface temperatures: Its relation to El Niño-southern oscillation events and dominant variation modes, *Int. J. Climatol.*, *25*, 913–930, doi:10.1002/joc.1172.

K. Hanawa and T. Horii, Department of Geophysics, Tohoku University, Sendai 980-8578, Japan.

T. Hasegawa, Oceanographic Research Department, Meteorological Research Institute, Japan Meteorological Agency, Nagamine 1-1, Tsukuba, Ibaraki 305-0052, Japan. (thasegaw@mri-jma.go.jp)